J Mater Sci: Mater Med (2008) 19:907–915
DOI 10.1007/s10856-007-0165-7

Enzyme-catalysed synthesis of calcium phosphates

Christiane Hoffmann · Cordt Zollfrank · Günter Ziegler

Received: 4 October 2006 / Accepted: 8 February 2007 / Published online: 1 August 2007

Abstract A biomimetic method is described for the precipitation of nanosized calcium phosphates using the alkaline phosphatase (EC 3.1.3.1), which is responsible for hydrolysis of organic and inorganic phosphates in vivo. Buffered solutions containing glycerol-2-phosphate and $CaCl_2$ in addition to $MgCl_2$ and the respective enzyme were prepared for calcium phosphate precipitation. The phosphate group of glycerol-2-phosphate was cleaved through enzymatic hydrolysis. The local inorganic phosphate concentration increased resulting in the precipitation of nanosized calcium phosphates phases (Ca–P phase) composed of calcium deficient hydroxyapatite (CDHA) and hydroxyapatite (HA). At high Ca^{2+}-concentration and large enzyme amounts mixed phases of HA/CDHA with an increasing quantity of HA were favoured. Under basic conditions (pH > 9) formation of HA was observed, whereas at neutral pH of 7.5 CDHA was primarily formed. The assignment of Ca–P phases was accomplished by FT-IR and Raman-spectroscopy in addition to X-ray diffractometry. The Ca–P materials exhibited BET surface areas of 173 m^2/g. SEM-micrographs of the Ca–P powders showed globular-shaped agglomerates of Ca–P particles. The size of the Ca–P crystallite ranged from 9 nm to 25 nm according to transmission electron microscopy (TEM), where round-shaped, platelike and fibrelike crystallites were found. All crystallites showed diffuse ring patterns in electron diffraction confirming the nanosize of the precipitate. Using the developed technique, it was possible to synthesise 100 g of bonelike Ca–P materials in 1 day using 15 L batches with optimised parameters.

C. Hoffmann · G. Ziegler
Friedrich-Baur-Research Institute for Biomaterials, University of Bayreuth, Ludwig-Thoma-Str. 36c, 95447 Bayreuth, Germany

C. Zollfrank (✉)
Department of Materials Science and Engineering – Glass and Ceramics, University of Erlangen-Nuremberg, Martensstr. 5, 91058 Erlangen, Germany
e-mail: cordt.zollfrank@ww.uni-erlangen.de

Introduction

The mineralisation of bone is a very complex physicochemical and biochemical process resulting in the deposition of hydroxyapatite within the collagen matrix. Up to now, biological calcium phosphate formation has not been understood in all details [1]. Because the concentrations of calcium and phosphate in the extracellular fluids are insufficient for spontaneous calcium phosphate precipitation, hydroxyapatite formation has been postulated to be initiated within extracellular matrix vesicles [2, 3]. These matrix vesicles contain a high amount of enzymes, particularly of alkaline phosphatases. Alkaline phosphatase has been suggested to be involved in hydroxyapatite formation by releasing phosphate groups by the hydrolysis of organic phosphates and pyrophosphate, which is an inhibitor of HA crystal growth [4–6]. In addition to proteins regulating the P homeostasis, further proteins (e.g. annexins) inside the vesicles are involved in Ca^{2+} homeostasis [2]. Once nucleated, HA crystals continue to grow inside the vesicles and they are released into the extracellular matrix when they achieve a definite size. The enzyme alkaline phosphatase is reported to be involved in the mineralisation process since Robinson proposed 1923 that this enzyme hydrolyses organic phosphates and the released inorganic phosphate precipitates with Ca^{2+} in form of calcium phosphate. However, the nature of the substrate

of the alkaline phoshatase within the body has not been clearly established [2, 4]. Alkaline phosphatases contain two tightly bound atoms of zinc and one of magnesium per monomer, which catalyse the non-specific hydrolysis of phosphate esters [7]. The class of alkaline phosphatases in general are present in a broad diversity in eukaryotic and prokaryotic organisms, suggesting that the non-specific hydrolysis of phosphate esters is functionally important, but the exact physiological role still remains a matter of discussion [8]. The hydrolysis reaction proceeds through a phosphoenzyme intermediate where a phosphorylated serine residue (Ser-102) at the active site was described. This was supported by the fact that the enzyme cleaves phosphate esters at identical rates irrespective of the leaving group or its pK [8, 9]. Several authors could demonstrate that alkaline phosphatase in combination with glycerophosphates initiates mineralisation processes of Ca–P phases [10–13].

Calcium phosphates are clinically used as bone substitute materials because of their excellent biocompatibility, bioactivity and osteoconductivity [14, 15]. For biomedical applications the preparation of calcium phosphates with given characteristics of particle morphology, stoichiometry, cristallinity and crystal size distribution is important, because small variations can lead to significant changes in the chemical, biological and physical behaviour of the material [16, 17]. In human hard tissue the mineral phase (biological apatite) is a non-stoichiometric hydroxyapatite containing several other ions like Mg^{2+}, Na^{+}, F^{-}, Cl^{-}, carbonate, etc. Therefore, it has been postulated over the last years, that biomaterials should consist of poorly crystalline and carbonate-substituted apatite [17]. Depending on the medical application, calcium phosphates with variable resorption properties are needed, which can be realised by using different calcium phosphates or mixed phases. Furthermore, in the last years there was an increasing interest in nanocrystalline calcium phosphate phases because of their higher specific surface and their higher chemical reactivity. These properties enable such materials for an application as delivery agent for drugs, proteins and DNA [18].

Various methods have been reported for the preparation of calcium phosphates, which can be divided into wet chemical methods (precipitation, hydrothermal technique and hydrolysis of other calcium phosphates) and solid-state reactions [14, 15]. The aim of the current work is to introduce a new synthesis method for the production of nanostructured calcium phosphates with variable resorption properties. By mimicking the calcium phosphate formation within the bone using alkaline phosphatase as enzyme and glycerol-2-phophate as substrate, it was possible to precipitate various calcium phosphate phases depending on the processing parameters. The effect of the variation of different process parameters on the resulting powders was studied.

Materials and methods

Formation of calcium phosphate phases by enzyme-catalysed hydrolysis of phosphate esters

The enzyme alkaline phosphatase (EC 3.1.3.1) from calf intestinal mucosa (1.5 units/mg; Fluka, Buchs, Switzerland) with a pH-optimum of 9.8 was used for the precipitation of Ca–P, Table 1. The lyophilised enzyme powder was dissolved in 1 ml of distilled water and subsequently poured into an optimised buffer solution containing 100 mmol/L tris(hydroxymethyl)aminomethane (TRIS, Merck, Darmstadt, Germany), 65 mmol/L glycerol-2-phosphate (Sigma-Aldrich, Steinheim, Germany) as the enzyme-substrate, 2.3 mmol/L $MgCl_2$ (Merck, Darmstadt, Germany), and $CaCl_2$ (Karl Roth, Karlsruhe, Germany). The used substrate concentration (65 mmol/L) was higher compared to the Michaelis–Menten constant for the enzymes, Table 1. As a consequence, the reaction rate will be near the maximum and independent on the substrate concentration. The pH of the buffer solution was adjusted with 1 M HCl to the respective experiment. The pH-value was kept constant during the reaction using an automated titrator unit (TitroLine alpha, Schott, Germany) and 1.0 M NaOH and 0.1 M NaOH, respectively. The precipitation experiments were performed with varying process parameters, such as Ca^{2+}-concentration, amount of enzyme, pH-value, and temperature. The detailed process parameters and the experimental data for the Ca–P phases formed during enzyme-catalysed hydrolysis are given in Table 2. After 48 h the solution was filtered, the obtained powder was washed twice with distilled water and dried at 100 °C. Afterwards the powders were sintered at 1250 °C for 1 h in air. A scaling-up to 15 L batches using the same molar concentrations of the components as above was successfully performed to synthesise 100 g of calcium phosphates by enzyme catalysed hydrolysis phosphate esters during 1 day.

Table 1 Source and properties of the enzymes used

Enzyme	Alkaline phosphatase EC 3.1.3.1
Organism	Calf, intestinal mucosa
pH-range	7.0...9.8...10.4
Activity (U)	15
K_M (mmol/L)	0.27
Molecular weight (kDa)	~60

Table 2 Summary of the varied process parameters and CaP-phases and specific surface areas of the precipitated powders

Enzyme	Amount of enzyme (mg/L)	Ca^{2+}-conc. (mmol/L)	pH/ temperature	CaP-phase	BET (m^2/g)
Alkaline	60	50	9.8/RT	HA/CDHA (5/95)	111
Phosphatase	60	90	9.8/RT	HA/CDHA (45/55)	197
	60	120	9.8/RT	HA/CDHA (58/42)	183
	60	90	7.5/RT	CDHA	142
	60	90	10.4/RT	HA	150
	180	50	9.8/RT	HA/CDHA (15/85)	144
	180	90	9.8/RT	HA/CDHA (40/60)	173
	180	90	9.8/37 °C	HA	121

Characterisation of the precipitated Ca–P phases

The Ca–P phases were analysed by FTIR/ATR-spectroscopy (Avatar 370, Thermo Nicolet, USA), Raman-spectroscopy (Labram, Horiba Jobin Yvon, France) and by X-ray diffractrometry (XRD 3000P Seifert, Germany). The composition of the mixed phases was semi-quantitatively estimated from the XRD-data and analysed using standard software (Diffracplus Eva, Bruker AXS, Germany). The particle size distribution was determined by a laser particle size analyser, which has a detection range from 40 nm to 500 μm (Cilas 1064, Quantachrome, Germany); these measurements were carried out in situ during the synthesis. The specific surface areas were measured by nitrogen adsorption (BET Gemini 2370, Micromeritics, Germany). The morphology of the particles was investigated by scanning electron microscopy (ESEM, Quanta 200, FEI, NL) operated at 25 kV. The Ca–P samples were analysed in a transmission electron microscope (TEM, Phillips CM 30, NL) operated at 300 kV. The particle sizes were determined from image analysis. Selected area electron diffraction (SAED) diagrams were recorded at a constant camera length of 1250 mm. The ring patterns were calibrated against polycrystalline aluminium.

Determination of enzyme catalytic activity

The activity of the enzymes is affected by many factors such as temperature, pH-value, and ionic concentration. In order to analyse the activity of the applied enzymes as a function of pH-value and temperature variation, the release phosphate ions in a Ca^{2+}-free buffer were measured according to the Fiske–Subbarow method [19]. The same buffer composition without $CaCl_2$ as described above was used. The enzyme activity was stopped by denaturation after 5 min through the addition of trichloroacetic acid. The absorption was measured at a wavelength of 340 nm by UV-spectroscopy (DU 640, Beckman Coulter, USA).

Results and discussion

Catalytic activity of the alkaline phosphatase

Alkaline phosphatase is a widely distributed non-specific phosphomonoesterase that functions through the formation of a covalent phosphoseryl intermediate [9]. It is a metalloenzyme with two Zn^{2+} and one Mg^{2+} at each active site [7]. The enzyme activity (here the rate of substrate conversion) is affected by several parameters such as amount of enzyme, pH-value, and temperature. Experiments without enzymes showed no release of phosphate and consequently precipitation of calcium phosphate could not be observed. Consequently, the glycerol-2-phosphate containing Ca^{2+} ions solutions could not be compared to the results obtained with enzyme containing mixtures. Figure 1 shows the measured relative activity of the alkaline phosphatase depending on the pH-value and the temperature. The pH-optima for the catalytic activity of the enzyme was 10.0 at RT and 9.8 at 37 °C. Consequently, the reaction rate with respect to the catalysed hydrolysis of the phosphate ester exhibited a peak under these optimised conditions. The release of phosphate ions from the glycerol-2-phosphate should be the largest for the optimum conditions of the calcium phosphate precipitation. However, the alkaline phosphatase also works with a decreased activity in a broad range of pH-values. Due to the enzymatic hydrolysis of the phosphate ester bond in glycerol-2-phosphate and the subsequent precipitation of calcium phosphate, a decrease of the pH-value depending on the precipitated Ca–P phase during the reaction takes place according to Eqs. 1 and 2. Six equivalents of protons (H^+) are produced in the case of CDHA formation whereas eight equivalents of H^+ appear in the case of HA-precipitation.

Formation of CDHA (Ca/P 1.50):

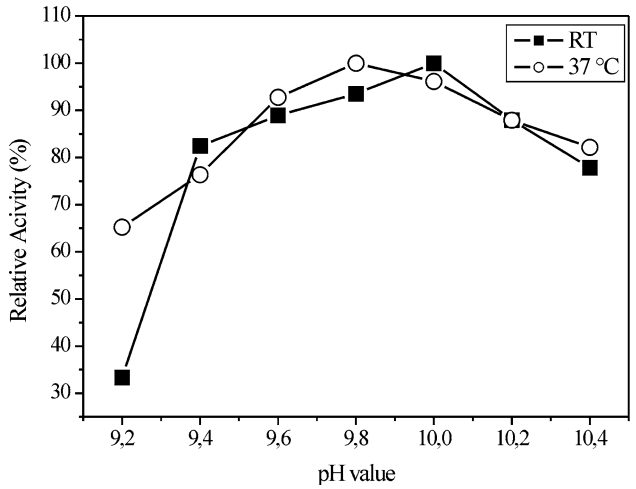

Fig. 1 Relative activity of the alkaline phosphatase as a function of pH-value and temperature (RT and 37 °C) after 5 min

$$6\text{R-OPO}_3 + 9\text{Ca}^{2+} + 7\text{H}_2\text{O} \rightarrow 6\text{R-OH} + \text{Ca}_9(\text{HPO}_4)(\text{PO}_4)_5\text{OH} + 6\text{H}^+ \quad (1)$$

Formation of HA (Ca/P 1.67):

$$6\text{R-OPO}_3 + 10\text{Ca}^{2+} + 8\text{H}_2\text{O} \rightarrow 6\text{R-OH} + \text{Ca}_{10}(\text{PO}_4)_6(\text{OH})_2 + 8\text{H}^+ \quad (2)$$

The pH-value of the solution was kept constant during the reaction using an automatic titrator unit and the spent amounts of base (1 M NaOH) were recorded as a function of the reaction time. The amount of the added base can be used as an indirect indicator of the enzyme activity: a high consumption of base refers a high hydrolysis rate followed by a fast Ca–P precipitation. It is assumed, that Ca–P precipitation occurs as soon as a phosphate ion is released by enzymatic hydrolysis of glycerol-2-phosphate. Thus, the influence of varied process parameters on the enzyme activity and the subsequent precipitation was analysed by plotting the volume of NaOH as a function of time, Fig. 2. In all cases, a nearly linear increase of the consumed NaOH can be observed until approximately 100 min. It was found that the initial rate did not depend on the amount of Ca^{2+}-ions at a given enzyme concentration, Fig. 2a. However, increasing the enzyme amount from 60 mg/L to 180 mg/L had a substantial effect on the initial reaction rate, which drastically increased with higher enzyme concentrations, Fig. 2a. This behaviour confirmed reports, where the rate of the Ca^{2+}-ions consumption is faster at increased phosphatase concentrations [11]. After prolonged reaction times ($t > 500$ min) the influence of Ca^{2+}-concentration became evident. Increasing the Ca^{2+}-concentration from 50 mmol/L to 90 mmol/L buffer yielded an increased reaction rate. The phosphatase was probably inhibited in the advanced

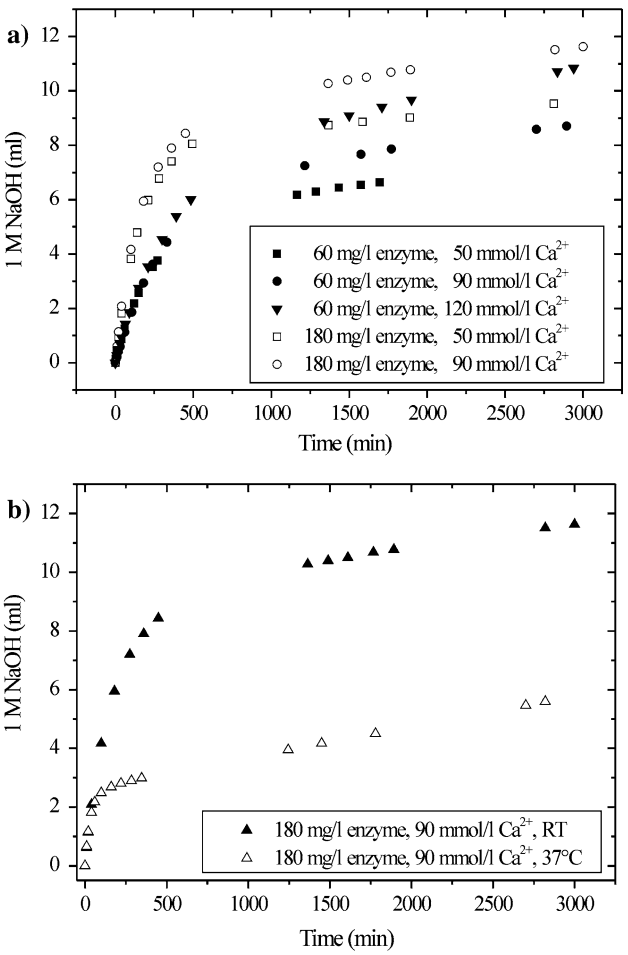

Fig. 2 (**a**) Calcium phosphate precipitation with alkaline phosphatase: plots of the NaOH-addition versus time for various enzyme amounts and the Ca^{2+}-concentration of the buffer, (**b**) Calcium phosphate precipitation with alkaline phosphatase: plot of the NaOH-addition versus time for different temperatures (RT and 37 °C)

stages of the reaction by phosphate ions, because they bind to the active site of the enzyme mutually reducing the hydrolysis rate of the glycerol-2-phosphate. As the Ca^{2+}-concentration was reduced during the precipitation of the Ca–P the concentration of free phosphate ions from substrate hydrolysis increased. The consumption of NaOH slowed down due to the competitive inhibition of the alkaline phosphatase.

Each enzyme has a temperature range in which a maximum rate of reaction is achieved; the reported temperature optimum of alkaline phosphatase is about 37 °C [20]. However, a distinct lower enzyme activity was observed at 37 °C than at 25 °C at a given constant Ca^{2+}- and enzyme concentration, Fig. 2b. Alkaline phosphatase is a metalloenzyme with binding sites for Zn^{2+} and Mg^{2+}. Leone et al. have shown that the activity of alkaline phosphatase can be modulated by Ca^{2+} [21]. At low concentrations of magnesium, calcium ions inhibit the enzyme activity by

displacing the magnesium ions. It might be possible, that at the given conditions this displacement was accelerated by a higher temperature followed by a lower enzyme activity.

Characterisation of the calcium phosphates

The variation of process parameter such as temperature and pH directly affects the precipitated Ca–P phase [22, 23]. Different experiments were conducted varying the enzyme concentration, the Ca^{2+}-ion concentration, the temperature and the pH-value. The results are summarised in Table 2. It was found, that the ratio of the fraction of HA/CDHA was sensitive to the parameters applied. At a fixed pH-value of 9.8 and RT with a given Ca^{2+}-concentration of 50 mmol/L primarily CDHA (95%) was formed. However, the HA/CDHA ratio increased from 5/95 to 15/85 with a threefold increased addition of enzyme from 60 mg/L to 180 mg/L. If the supply of Ca^{2+}-ions was increased to 90 mmol/L the HA/CDHA ratio was 45/55 for 60 mg/L enzyme and 40/60 for 180 mg/L enzyme, respectively. Thus, with rising the Ca^{2+}-concentration a higher HA amount was obtained. Variation of the pH-value to neutral (7.5) at a constant temperature (RT) and fixed amounts of enzyme resulted in the sole formation of CDHA, whereas at higher pH-values (10.4) HA was exclusively obtained. The temperature also had an effect on the Ca–P phase formation. Increasing the temperature to 37 °C yielded HA as the only phase at high enzyme concentrations and sufficient Ca^{2+}-ion supply.

The precipitated and sintered (1250 °C) Ca–P powders were characterised by Raman-spectroscopy, Fig. 3. Ca–P powders can be identified by the position of the strong υ_1 band in the range of 950–985 cm^{-1} [24, 25]. The spectrum of hydroxyapatite exhibited a strong characteristic PO_4^{3-} band at 962 cm^{-1}, whereas TCP shows two characteristic bands at 948 cm^{-1} (HPO_4^{2-}) and at 970 cm^{-1} (PO_4^{3-}) [26]. To differentiate the two phases the as-precipitated powders were sintered (1250 °C) and CDHA transformed during the thermal treatment to TCP [27]. Thus, the sole presence of TCP in the Raman-spectrum of Ca–P powders obtained at a pH-value of 7.5 after heat treatement confirmed that the precursor material was CDHA as indicated above. At a pH-value of 9.8 a mixture of TCP and HA was detected, which is in good agreement with the results described above. After sintering Ca–P powders which were obtained at a pH-value of 10.4 only HA was observed in the corresponding Raman-spectrum, Fig. 3a. The formation of HA after sintering was also observed for Ca–P powders, which were synthesised at 37 °C, Fig. 3b. The sintered Ca–P powders from samples obtained at RT were composed of a mixture of TCP and HA as expected.

SEM-micrographs of Ca–P powders prepared with alkaline phosphatase are shown in Fig. 4. The powders appear as agglomerated Ca–P nanoparticles, which have a more or less globular shape. Ca–P agglomerates with sizes ranging from 10 µm to 40 µm were observed for Ca–P precipitation obtained at a pH-value of 7.5, Fig. 4a. Smaller Ca–P agglomerates with diameters from 1 µm to 15 µm were found for Ca–P powders generated at high pH-value (10.4) with constant Ca^{2+}-concentration of 90 mmol/L, Fig. 4b. It was interesting, that increasing the pH-value (7.5...9.8...10.4, Fig. 4a,b,d) or a low Ca^{2+}-concentration (50 mmol/L, Fig. 4c) resulted in smaller calcium phosphate agglomerates. An increase of the amount of enzyme led to an increase of precipitation sites. In this case the agglomerates were less globular shaped, extremely microstructured, but generally larger in size (not shown here).

The TEM-investigation revealed, that the Ca–P precipitation resulted in round-shaped, platelike crystallites with dimensions from 7 nm to 30 nm, depending on the conditions

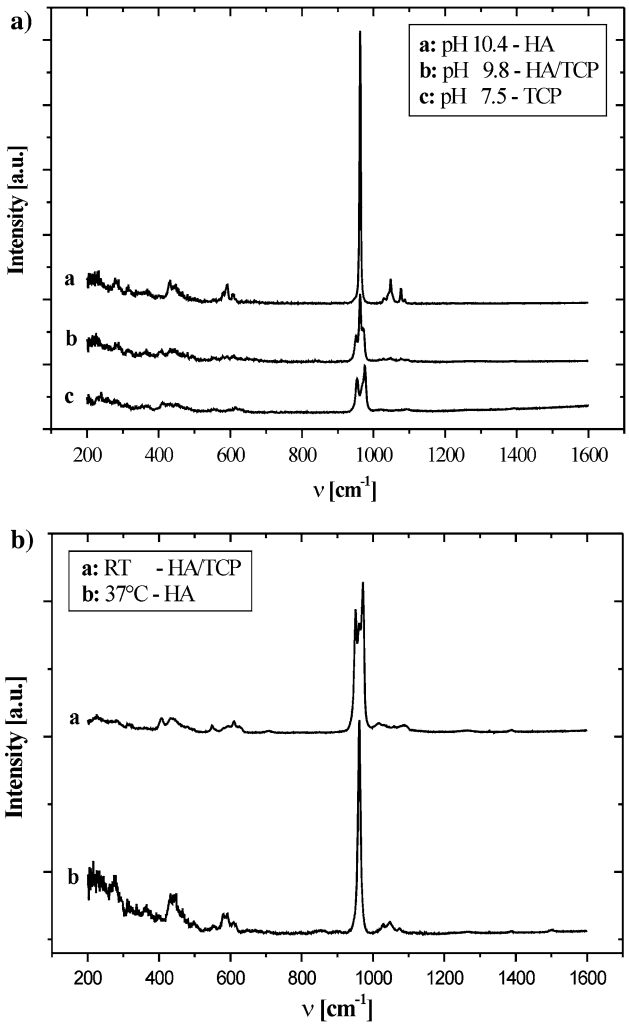

Fig. 3 (**a**) Raman-spectra of sintered (1250 °C) powders precipitated with alkaline phosphatase (60 mg/L enzyme and 90 mmol/L Ca^{2+}) at different pH-values, (**b**) Raman-spectra of sintered (1250 °C) powders precipitated with alkaline phosphatase (60 mg/L enzyme and pH 9.8) at different temperatures (RT and 37 °C)

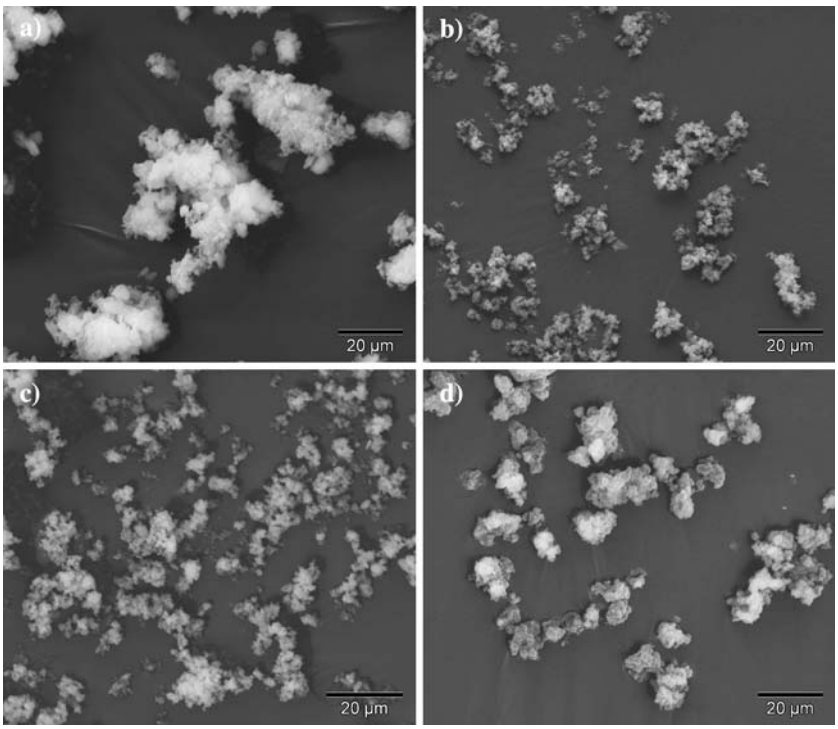

Fig. 4 SEM-micrographs of Ca–P powders precipitated at RT with alkaline phosphatase (60 mg/L) obtained at different pH-values (**a**,**b**,**d**) and different Ca^{2+}-concentrations (**c**,**d**): (**a**) 90 mmol/L Ca^{2+}, pH 7.5, (**b**) 90 mmol/L Ca^{2+}, pH 10.4, (**c**) 50 mmol/L Ca^{2+}, pH 9.8 and (**d**) 90 mmol/L Ca^{2+}, pH 9.8

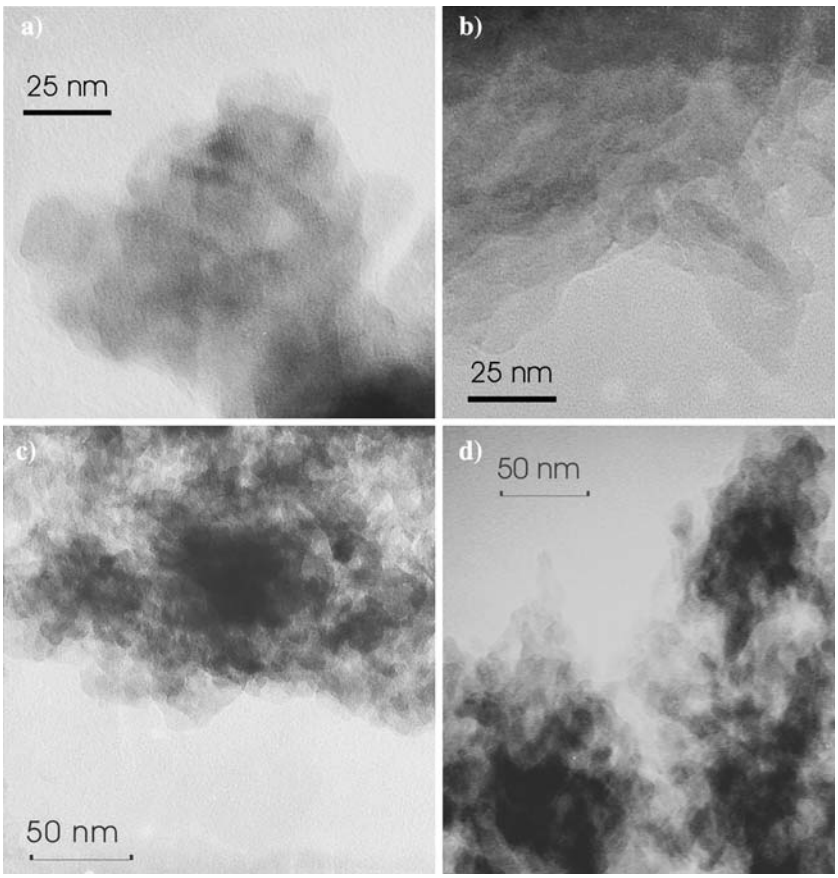

Fig. 5 TEM-micrographs of Ca–P powders precipitated at constant pH-value (9.8) with alkaline phosphatase obtained at different Ca^{2+}-concentrations (**a**,**b**), different enzyme amounts (**b**,**c**) and different temperatures (**c**,**d**): (**a**) 60 mg/L enzyme, 50 mmol/L Ca^{2+}, RT, (**b**) 60 mg/L enzyme, 90 mmol/L Ca^{2+}, RT, (**c**) 180 mg/L enzyme, 90 mmol/L Ca^{2+}, RT and (**d**) 180 mg/L enzyme, 90 mmol/L Ca^{2+}, 37 °C

applied, Fig. 5. If the amount of CDHA was high as in the case of pH 9.8 and a Ca^{2+}-concentration of 50 mmol/L the observed crystallite size was approximately 24 ± 6 nm, whereas the crystallite size decreased with higher supply of Ca^{2+}-ions to 10 ± 3 nm during enzymatic hydrolysis, Fig. 5a,b. The mean crystallite size further decreased to

approximately 9 nm, if the enzyme concentration was increased (Fig. 5b,c) or if the precipitation temperature was raised from 25 °C to 37 °C, Fig. 5c,d. It should be noted that, all precipitated Ca–P powders exhibited broad rings in selected area diffraction patterns, which could be assigned to the principal reflections of hydroxyapatite phases. A distinction between CDHA and HA was not possible by means of electron diffraction.

Measurements of the particle size distribution in the range from 40 nm to 500 µm were performed in situ during the enzymatic hydrolysis of the glycerol-2-phosphate, Fig. 6a. The observed bimodal curves were typical for all experiments carried out with alkaline phosphatase. However, the small intensity increase below 40 nm is attributed to an artefact of the instrument, because particles smaller than 40 nm could not be resolved. In any case, neither the variation of process parameters nor the prolonged reaction time caused a significant change of the curve shape and peak position located in the micrometer range. The influence of the process parameters on the particles sizes is shown in Fig. 6b. The d_{50}-sizes varied between 4.25 µm and 8 µm. However, the d_{50}-particle sizes increased with a lower or higher Ca^{2+}-concentration than 90 mmol/L (standard) and a lower pH-value (8.5). A higher amount of enzyme (180 mg/L) resulted only in a small increase in particle size.

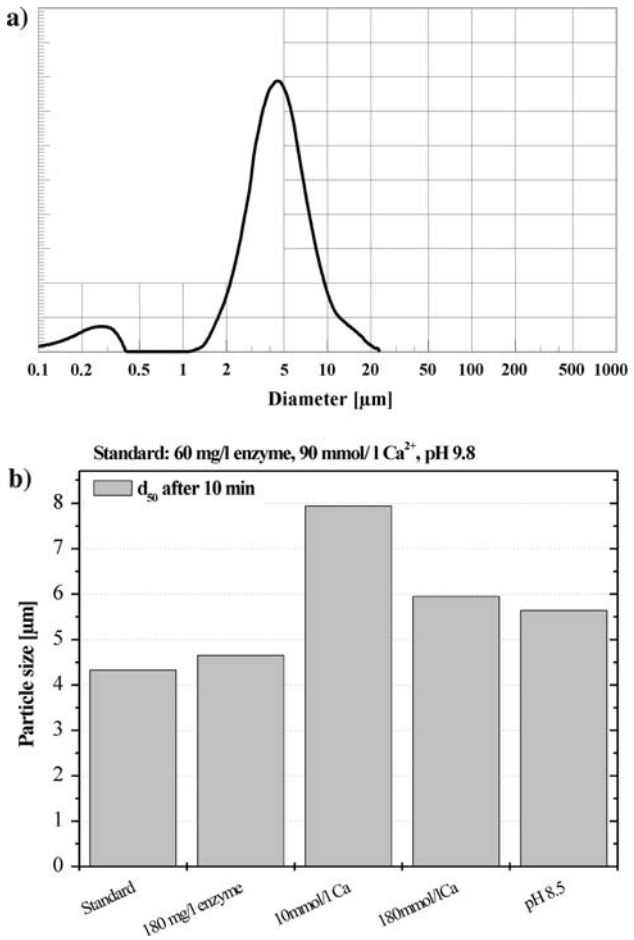

Fig. 6 (**a**) Particle size distribution from in situ measurement after 10 min (60 mg/L enzyme, 90 mmol/L Ca^{2+} and pH 9.8), (**b**) Particle size distribution in situ measurements (d_{50} after 10 min, without ultrasonic treatment); the variations of the standard condition (60 mg/L enzyme, 90 mmol/L Ca^{2+}, pH 9.8) are given above

Early work on enzyme catalysed hydrolysis on water-soluble glycerol-2-phosphate showed the oriented assembly of Ca–P platelets on collagen tapes, which were modified with enzymes [28]. However, precipitation of Ca–P phases using alkaline phosphatase from calfskin was performed at a pH-value of 8.5, where an immediate Ca–P formation was not observed. The samples were soaked for 24 h after which formation of apatitic materials was occurred. The experiments were repeated [13] with alkaline phosphatase, probably from bovine intestinal mucosa, from loaded reconstituted collagen templates. The Ca–P particle grew on the collagen fibres within 2 weeks. In another study, collagen sheets loaded with alkaline phosphatases from bovine intestinal mucosa were applied at a pH-value of 9 [11]. The collagen sheets were incubated up to 6 h at 37 °C. The Ca–P particles observed, exhibited a globular shape with dimensions of approximately 200 nm. Enzymes which are immobilised to template structures decrease in their catalytic activity, since they are covered by the growing Ca–P layer [11, 13, 28]. In our study, the enzyme was used in the dissolved state, that means, that after hydrolysing and release of a substrate, the enzyme is available for additional substrates, and the reaction continuously proceeds. However, the hydrolysis rate decreased with consumed amounts of either the substrate glycerol-2-phosphate or the Ca^{2+}-ions. The nanosized Ca–P particle appeared strongly agglomerated. The Ca–P phase formation was influenced by the conditions. At the neutral pH-value and low substrate concentrations, CDHA was the principal phase, whereas primarily HA was formed at high pH-values from 9.8 to 10.4, large substrate concentrations and increased temperature. It could be shown, that the crystallite size varied with the phase composition of the precipitated Ca–P powders, Fig. 7a. If CDHA was the principal phase, the individual crystallite sizes observed were distributed around 24 nm. With an increase of the HA/CDHA ratio the crystallite size decreased to approximately 9 nm. The reaction was performed in solution leading to Ca–P powders with large surface areas. At the pH-optimum of 9.8, where the alkaline phosphatase displayed the highest activity, the highest specific surface area of 197 m^2/g of the precipitated powder was measured. An increase or decrease of this pH-optimum of 9.8 resulted in Ca–P powders with lower surfaces. Furthermore, the specific surface area decreased also with rising temperature

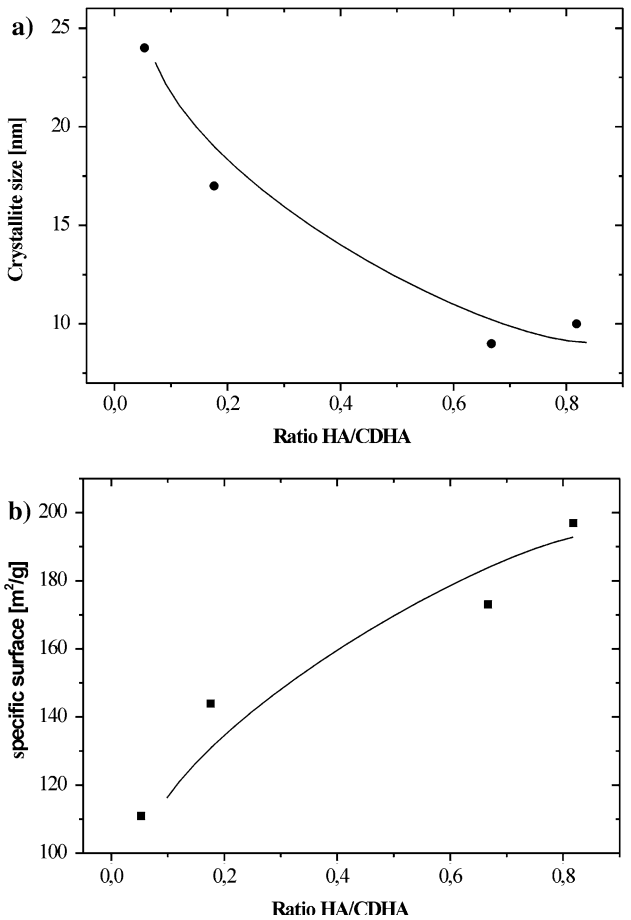

Fig. 7 (**a**) Particle size of the enzymatic synthesised Ca–P powders as a function of HA/CDHA ratio, (**b**) specific surface area of the Ca–P powders as a function of HA/CDHA ratio; the lines are drawn as a guide for the eye

(RT: 173 m^2/g, 37 °C: 121 m^2/g) as it was notified by other authors [29]. However, it should be noted, that the measured specific surfaces area rose as the ratio of HA/CDHA also increased, Fig. 7b. If the powder is primarily composed of CDHA, a surface area of approximately 110 m^2/g was observed, which gradually increased with the HA/CDHA ratio up to 195 m^2/g. The measured results confirmed the observation on crystallite size deduced from the TEM-investigation, that smaller crystallite sizes yield a higher surface area, Fig. 7a,b.

Conclusions

It could be shown that the local release of phosphate by an enzyme-catalysed reaction in an opitimated buffer solution initiated the precipitation of nanostructured calcium phosphates. This synthesis method imitated the calcium phosphate precipitation within the bone using glycerol-2-phopshate as substrate for phosphate release applying the enzyme alkaline phosphatase. The utilisation of the enzyme alkaline phosphates allowed the precipitation of pure (CDHA and HA) or mixed phases with varying CDHA/HA-ratios. In addition to the pH-value, the variation of various other process parameters like the amount of enzyme, Ca^{2+}-concentration and temperature, directly influenced the precipitated phases and other characteristics of the precipitated powders. Furthermore, some process parameters had an effect on the enzyme activity and thus indirectly on the synthesised calcium phosphates.

Acknowledgment The TEM-work was carried out at the Central Facility for High-Resolution Electron Microscopy of the Friedrich-Alexander of University Erlangen-Nuremberg, Germany.

References

1. A. L. BOSKEY, *J. Cell. Biochem. Suppl.* **30/31** (1998) 83
2. M. BALCERZAK, E. HAMADE, L. ZHANG, S. PIKULA, G. AZZAR, J. BANDOROWICZ-RADISSON, J. PIKULA and R. BUCHET, *Acta Biochim. Polonica* **50** (2003) 1019
3. H. C. ANDERSON, *Lab. Invest.* **60** (1989) 320
4. R. ROBINSON, *Biochem. J.* **17** (1923) 286
5. M. P. WHYTE, *Endocr. Rev.* **15** (1994) 439
6. S. Y. ALI. In *Bone: biology and skeletal disorders*, edited by C. C. Whitehead, (Carfax Publishing Co.: UK, 1992) p. 19ff
7. E. E. KIM and H. W. WYCKOFF, *J. Mol. Biol.* **218** (1991) 449
8. A. CHAIDAROGLOU, D. J. BREZINSKI, S. A. MIDDLETON and E. R. KANTROWITZ, *Biochemistry* **27** (1988) 8338
9. J. H. SCHWARTZ and F. LIPMANN *Proc. Natl. Acad. Sci. USA* **47** (1961) 1996
10. N. FRATZL-ZELMAN, P. FRATZL, H. HÖRANDER, B. GRABNER, F. VAGRA, A. ELLINGER and K. KLAUSHOFER, *Bone* **23** (1998) 511
11. K. YAMAUCHI, T. GODA, N. TAKEUCHI, H. EINAGA and T. TANABE, *Biomaterials* **25** (2004) 5481
12. R. FILMON, F. GRIZON, M. F. BASLÉ and D. CHAPPARD, *Biomaterials* **23** (2002) 3053
13. Y. DOI, T. HORIGUCHI, Y. MORIWAKI, H. KITAGO, T. KAJIMOTO and Y. IWAYAMA, *J. Biomed. Mater. Res.* **31** (1996) 43
14. W. SUCHANEK and M. YOSHIMURA, *J. Mater. Res.* **13** (1998) 94
15. M. VALLET-REGÍ and J. M. GONZÁLEZ-CALBET, *Prog. Solid State Chem.* **32** (2004) 1
16. J. GÓMEZ-MORALES, J. TORRENT-BURGUÉS, T. BOIX and J. FRAILE, *Cryst. Res. Technol.* **36** (2001) 15
17. D. TADIC, F. PETERS and M. EPPLE, *Biomaterials* **23** (2002) 2553
18. P. N. KUMTA, C. SFEIR, D. H. LEE, D. OLTON and D. CHOI, *Acta Biomater.* **1** (2005) 65
19. C. H. FISKEA and Y. SUBBAROW, *J. Biol. Chem.* **66** (1925) 375
20. V. LUSTIG and J. A. KELLEN, *Comp. Biochem. Physiol., B Biochem. Mol. Biol.* **39** (1971) 311
21. F. A. LEONE, P. CIANCAGLINI and J. M. PIZAURO, *J. Inorg. Biochem.* **68** (1997) 123
22. C. LIU, Y. HUANG, W. SHEN and J. CUI, *Biomaterials* **22** (2001) 301
23. H. ZHANG, Y. WANG, Y. YUHUA and S. LI, *Ceram. Inter.* **29** (2003) 413

24. J. D. PASTERIS, B. WOPENKA, J. J. FREEMAN, K. ROGERS, E. VALSAMI-JONES, J. A. M. VAN DER HOUWENA and M. J. SILVA, *Biomaterials* **25** (2004) 229
25. G. PENEL, G. LEROY, C. REY and E. BRES, *Calcif. Tissue Int.* **63** (1998) 475
26. S. KOUTSOPOULOS, *J. Biomed. Mater. Res.* **62** (2002) 600
27. R. Z. Legeros. In *Monographs in Oral Science*, vol. 15, (Karger: Basel)
28. E. BANKS, S. NAKAJIMA, L. C. SHAPIRO, O. TILEVITZ, J. R. ALONZO and R. R. CHIANELLI, *Science* **198** (1977) 1164
29. L. M. RODRÍGUEZ-LORENZO and M. VALLET-REGÍ, *Chem. Mater.* **12** (2000) 24